Electronic structure of antimony-doped tin oxide

K. C. Mishra
Central Research, Osram Sylvania Inc., 100 Endicott Street, Danvers, Massachusetts 01923

K. H. Johnson
Department of Materials Science, Massachusetts Institute of Technology, Cambridge, Massachusetts 02139

P. C. Schmidt
Institut Für Physikalische Chemie, Technische Hochschule Darmstadt, Darmstadt, Germany
(Received 1 February 1995)

The electronic structure and associated properties of antimony-doped tin (IV) oxide have been studied using both the self-consistent-field scattered-wave molecular-orbital cluster approach and the augmented-spherical-wave supercell band-structure approach. The calculated molecular-orbital energy eigenvalues and wave functions have been used to interpret several interesting optoelectronic properties of this defect semiconductor. The nature and origin of the energy gap from optical-absorption studies and the valence-band structure from ultraviolet photoelectron spectroscopy (UPS) have been satisfactorily explained using the band structure of pure and antimony-doped tin oxide. It is observed that the antimony ion leads to an impurity band in the band gap and increases the forbidden gap of the host material. This partially filled free-electron-like band is the origin of the UPS peak near the band edge whose intensity grows with the dopant concentration.

I. INTRODUCTION

Tin (IV) oxide is a semiconductor with many interesting optoelectronic properties. Tin oxide with a high dopant concentration of antimony exhibits quasimetallic conductivity while maintaining its transparency in the optical region.[1] This interesting optoelectronic property is exploited in solar cells and optical devices.[2] The mixed oxides of antimony and tin are often used as catalysts in the oxidation and ammoxidation of hydrocarbons, namely propylene to acrolein and acrylonitrile.[3–5] It is believed that the surface chemical composition critical to catalytic properties differs significantly from that of the bulk;[6] therefore, considerable attention has been paid to analyzing the surface composition and segregation of antimony atoms by surface-sensitive techniques.[7–9]

The physics of group-V impurities in group-IV semiconductors is fairly well understood in terms of the band structure of the bulk material and the donor levels from these impurities and subsequent n-type conductivity of these materials. One can explain the quasimetallic behavior of tin oxide using a similar picture, but its transparency in the visible region presents a conceptual difficulty that requires a careful consideration of this material as an ionic system with impurity states. In ionic crystals, the effect of a similar substitution on the electronic structure is usually interpreted in terms of localized defect levels with an accompanying charge-compensating mechanism to stabilize the valence state of the dopant ion. Because of the charge compensation, the impurity levels are usually empty with no conduction electrons, thus retaining most of the characteristics of the host material. For example, one may consider a pentavalent antimony ion at a tetravalent tin site being charge compensated by cation vacancies. The extra electron contributed by antimony compensates for the absent tetravalent ion in fulfilling the valence of the oxygen ions, i.e., in maintaining a filled valence band. The multiple valency of antimony can provide an alternate scenario of charge compensation without cation vacancies. In fact, Mossbauer studies[6] have indicated segregation of trivalent ions in the surface layer and pentavalent ions in the bulk, suggesting an effective valence of 4. Tin oxide doped with antimony presents a real challenge to electronic-structure calculation in order to explain its optoelectronic properties, since the explanations must transcend formal descriptions of a material in terms of ionic and semiconducting properties.

The electronic structure of pure tin oxide has been studied extensively by various theoretical[10–12] and experimental studies in the past.[13–17] In this paper, we have extended the electronic-structure calculations to include the antimony ions in tin oxide. Similar to our previous works on defects in ionic crystals,[18] both the real-space cluster approach and the k-space band-structure approach have been used in a complementary manner to develop a consistent picture of its electronic structure. Beginning with pure tin oxide, the changes in the electronic structure of the host material due to the presence of the antimony atom has been traced through cluster and band-structure calculations. It will be shown that the antimony atoms in tin oxide lead to an impurity band with a significant free-electron-like character that provides a satisfactory explanation for many of its interesting optoelectronic properties.

II. THEORY

A. Structure

Tin oxide crystallizes in the rutile structure with two formula units per unit cell, the space group symmetry being $P4_2/mnm$, with a and c lattice constants being 4.737 and 3.186 Å.[19] Every unit cell contains two formula units of SnO_2 with tin and oxygen atoms occupying the Wyckoff positions a and f. The site symmetry of the tin atoms is D_{2h}. Cluster calculations were performed using these structural parameters to generate the positions of atoms in the clusters while retaining the site symmetry in all the cases. Additionally, calculations were also performed assuming higher-order symmetry groups to develop an understanding of how the degeneracy of various molecular orbitals are removed. The band-structure calculation for pure tin oxide is performed using the conventional unit cell as the building unit. For the supercell calculation, the lattice constant c is doubled to define a supercell which includes two old primitive cells in which one of the tin atoms was replaced by an antimony atom corresponding to an impurity concentration of 8 at. %. This is comparable to the antimony concentration in tin oxide for optimal catalytic activity.

B. Computational procedure

The calculations are performed using the scattered-wave molecular-orbital (SW-$X\alpha$) method[20] and the augmented-spherical-wave (ASW) band-structure method.[21] The cluster results are based on three different clusters: a tin-centered cluster with six nearest neighbors; a cluster containing two tin atoms and ten oxygen atoms with the two tin atoms being located on the c axis of the crystal; and a cluster similar to the second one with an antimony atom replacing one of the tin atoms. The calculations are repeated with different exchange potential approximations, but the energy eigenvalues change by less than 1%. The results presented in this work derive mostly from calculations based on the $X\alpha$ approximation of the exchange correlation potential.

The band-structure calculations are done using the Hedin-Lundquist exchange-correlation potential.[22] In the ASW procedure, the unit-cell volume is partitioned into overlapping atomic spheres, the sphere radii being critical in the determination of the energy gaps. However, the overall features of the bands do not change with the sphere radii, and the radii are in most cases transferable. In the present calculation, we have used atomic spheres of radii 1.24 and 1.30 Å for the tin and oxygen atoms, respectively. Additionally, empty spheres of radius equal to 0.87 and 0.76 Å are placed at the Wyckoff position c and f, respectively, to fill up the empty space. The present choice of sphere radii not only gives the correct optical gap but also reproduces the essential features of the valence band as revealed by the ultraviolet photoemission spectroscopy (UPS) measurements. These radii are subsequently used for the supercell calculation including the antimony atom, its sphere radius being chosen to be the same as that for tin.

III. RESULTS AND DISCUSSION

A. Cluster calculation

The electronic structure of pure tin oxide is studied using two clusters: one consisting of seven atoms, with the tin atom being at the center, and the other centered between two tin atoms on the c axis with 12 atoms. In the first calculation, the crystallographic a axis coincides with the z axis of the cluster, while in the second the crystallographic c axis is the z axis of the cluster. For all clusters studied in this work, the standard embedding scheme with a Watson sphere is used. The $4d$, $5s$, and $5p$ orbitals of tin and $2s$ and $2p$ orbitals of oxygen are treated as valence orbitals. The molecular energy levels composed of oxygen $2s$- and $2p$-like states and the $4d$-like orbitals of tin appear as bands separated by well-defined gaps. The highest occupied molecular-orbital (HOMO) level composed predominantly of oxygen $2p$-like states belongs to the b_{1g} representation of the D_{2h} point group with a significant admixture of the tin $4d$-like orbital. The lowest unoccupied molecular orbital (LUMO) belongs to the a_g representation and is composed tin $5s$-like and oxygen $2p$-like states indicating strong covalency and delocalization of the conduction-band states. The HOMO-LUMO separation is calculated to be 5.3 eV. However, an optical transition between a_g and b_{1g} states is not allowed. The lowest-energy allowed transition corresponds to an excitation from a b_{3u} level with significant Sn $5p$-like character to the LUMO at 6.07 eV. This transition corresponds to the optical excitation across the energy gap. However, the calculated gap is approximately 60% greater than the observed gap [3.8 eV (Ref. 17)]. This is partly due to perturbations caused by four levels (b_{1g}, a_g, b_{3g}, and b_{2g}) at the top of the valence band with significant mixing with tin d-like character that are mostly associated with the surface states of the cluster.

The width of the oxygen $2p$-like band, i.e., the width of the energy interval containing discrete molecular orbitals associated with the oxygen $2p$-like states for this cluster, is found to be 4.8 eV, indicating the strong covalency of the system. The gap between the oxygen $2p$-like band and $2s$-like band, and between the oxygen $2s$-like band and tin $4d$-like band, are found to be 9.9 and 3.1 eV. The tin $4d$-like band has a very narrow bandwidth (0.5 eV), indicative of the localized nature of these states.

Our past experience with ionic crystals has been that one does not really need very large clusters to explain the optical properties. This is because photoexcitation of electrons in solids is a local process and therefore depends largely on the local electronic structure. However, in the present case, the discrepancy between the observed and predicted values is large, and the degree of covalency is very strong, which prompted us to study a larger cluster consisting of 12 atoms including two tin atoms to determine the extent of second-nearest-neighbor interaction. For this cluster, the LUMO and HOMO levels belonged to a_g and b_g representations (note the different orientations of the clusters mentioned earlier) with a separation of 2.3 eV. The *ungerade* molecular orbital with significant Sn p character is found to be a b_{3u} orbital at

3.2 eV below the LUMO level. This compares reasonably well with the observed gap for tin oxide (3.8 eV). The band widths and band gap also change with the increased cluster sizes, but less severely: the oxygen $2p$-like bandwidth increases to 5.6 eV, the bandwidths of oxygen $2s$-like bands and tin $4d$-like bands increase from 1.8 and 0.5 eV to 2.6 and 0.6 eV, respectively, and the gaps between the oxygen $2p$-like and $2s$-like bands and oxygen $2s$-like band and tin $4d$-like bands change to 8.9 and 3.8 eV. These changes in most cases reflect a better agreement with experimental data, to be discussed later in the text.

The effect of antimony substitution is studied using a cluster similar to the 12-atom cluster described earlier, with one of the tin atoms being replaced by an antimony atom in a pentavalent state which lowers the site symmetry to C_{2v}. The LUMO level (a_1) is found to have significantly more antimony $5s$-like character. The next-higher level is an antibonding combination of tin and antimony $5s$-like states in b_1 representation. The separation between these levels is 0.7 eV, suggesting that antimony introduces a donorlike level. This separation is expected to decrease when the LUMO is occupied by an electron, indicating that the ionization energy associated with this donor state is less than 0.7 eV. The band-gap transition is found to be 3.3 eV, corresponding to an excitation from a b_1 level in the valence band to the a_1 donor state. This is comparable to the band gap (3.2 eV) obtained for the pure tin oxide calculated from the earlier cluster, indicating that the impurity level perturbs the local electronic structure, leading to an increase in the band gap of the host system. However, the donor level remains practically at the same place on the energy scale where the bottom of the conduction band of the pure tin oxide used to be. This feature is confirmed by the band-structure calculation discussed below.

A number of changes are also noted in the energy-level structure of this cluster compared to the pure tin oxide cluster. The band widths of the oxygen p-like, oxygen $2s$-like, and tin $4d$-like bands increase to 7.3, 3.3, and 0.5 eV. The gaps between the oxygen $2p$-like, oxygen $2s$-like, and tin $4d$-like bands are found to be 7.0 and 3.2 eV. The antimony $4d$-like band appears 9.3 eV below the tin $4d$-like band. Significant admixture of the tin or antimony $5s$-like states is observed in the deep valence-band levels.

B. Band-structure calculation

The band structure calculated for the pure tin oxide is shown in Fig. 1, and has features similar to those reported by Robertson.[12] The Fermi level is chosen to be the zero of the energy scale. The ordering of the energy bands is similar to that in the cluster calculation, i.e., the oxygen $2p$-like, oxygen $2s$-like, and tin $4d$-like bands (not shown in Fig. 1) follow the same ordering as the corresponding molecular orbitals. The conduction band exhibits significant free-electron-like character in the Δ direction (Γ-X direction) or Λ direction (Γ-M direction), unlike the band structure reported by Jacquemin and Brodure.[11] The minimum gap is observed at the Γ point, the direct gap being 3.7 eV. The present results do not indicate the presence of any lower indirect gap. The

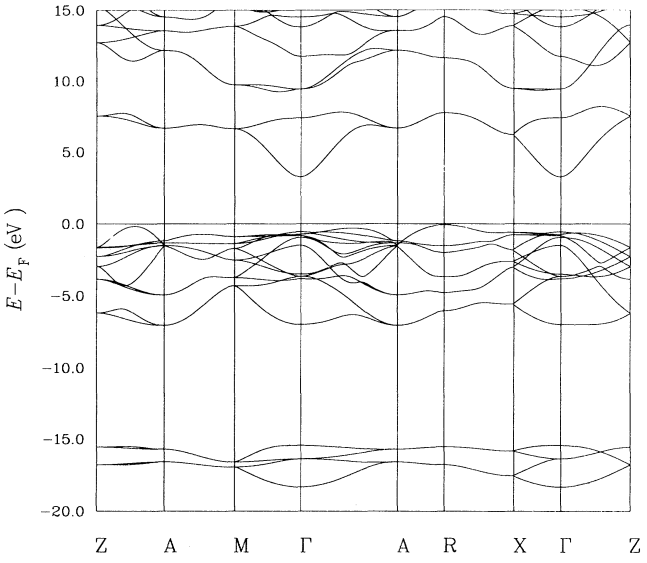

FIG. 1. The band structure of SnO_2. The zero of the energy scale is the Fermi energy E_F.

band gap of tin oxide has been measured by a number of workers, and varies from 4.3 to 2.25 eV,[13–17,11] which is possibly due to variations in the purity of samples. The most probable value is 3.89 eV,[11] which agrees very well with the calculated gap from the band structure and the cluster calculation. The analysis of the partial density of states (Fig. 2) suggests the band-gap transition involves

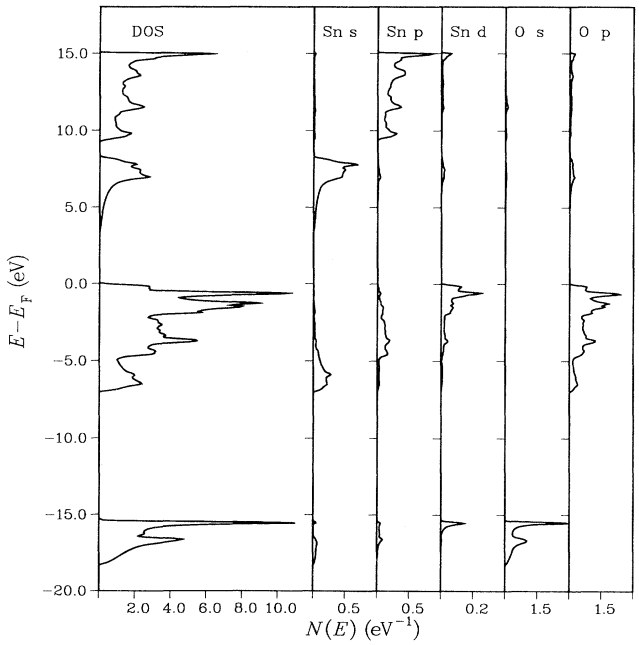

FIG. 2. The density of states (DOS) of SnO_2. The first column shows the total density of states. The following columns contain the partial densities and consecutively, the s-, p-, and d-like partial DOS of Sn and the s- and p-like DOS of O.

excitations from an oxygen $2p$-like state to tin s-like conduction-band states. The density of states plotted in Fig. 2 indicates a bandwidth of 7.0 eV, which is comparable to the p bandwidth from the cluster calculation and also to that reported from the UPS measurements [$\sim$10.0 eV (Refs. 7–9 and 23)]. The three peaks associated with the valence band appear at 4.3, 7.3, and 11.1 eV, which compare well with the UPS peaks at 4.8, 7.4, and 11.2 eV.[8] The partial-density-of-states calculation indicates a significant admixture of tinlike states deep inside the valence band.

In Fig. 3 we show the band structure of the Sn_3SbO_8 system. In this calculation, we have assumed no charge compensation; therefore one expects that this system will be metallic with one of the low-lying states half-filled. The question is whether this is a predominantly antimonylike or tinlike band. In the latter case, one can think of the antimony atoms donating their last electron to the tinlike state, and the conductivity is essentially due to a tinlike conduction band as speculated in Ref. 9. In the former case, two things may happen. We may get an impurity band in the gap which is very localized and half-filled. Thus one will need to supply energy to excite these electrons to a free-electron-like conduction band with significant tin character, and the conduction will be due to the electrons in this band. This would give a semiconductorlike behavior with an activation energy. Alternatively, the donor band itself may be free-electron-like and give the conductive properties of the material. Of course, it would exhibit a quasi-semiconductor-like behavior corresponding to excitation of electrons to the tinlike band. The last case appears to be true. An additional band (Fig. 3) appears in the forbidden gap with free-electron-like character near the Γ point. The

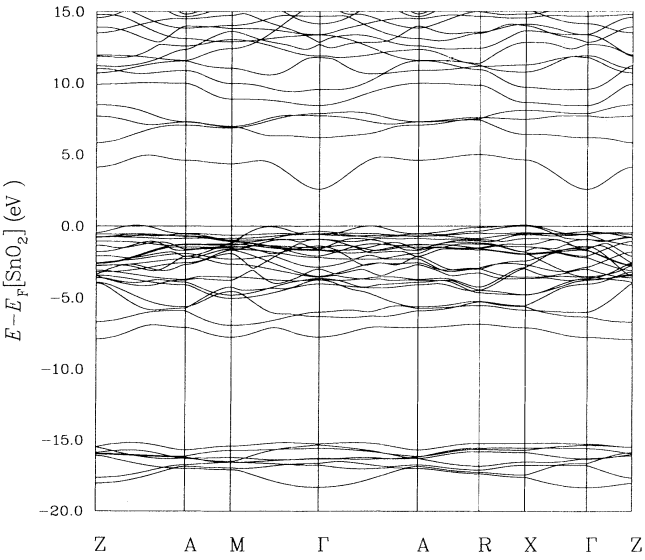

FIG. 3. The band structure for lines of symmetry in the Brillouin zone of Sn_3SbO_8. The Fermi energy E_F of SnO_2 is the zero of the energy scale.

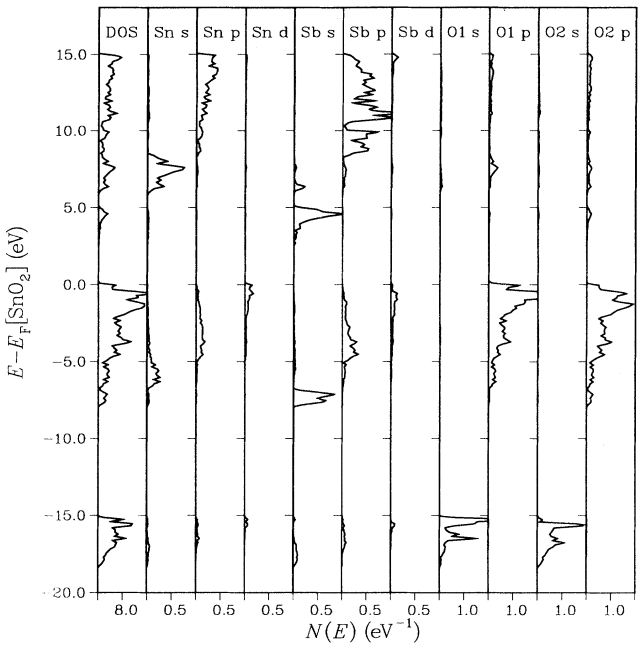

FIG. 4. The density of states (DOS) of Sn_3SbO_8. The first column shows the total density of states. The following columns contain the partial densities, consecutively the s-, p-, and d-like partial DOS of Sn, the s-, p-, and d-like partial DOS of Sb, and the s- and p-like DOS of O_1 and O_2.

partial-density-of-states calculation indicates that the electronic states associated with this band have antimony $5s$-like character (Fig. 4), which mixes more strongly with the oxygen $2p$-like states than with the tin $5s$-like state. The gap near the Γ point is 2.9 eV, the Fermi level being 4.1 eV above the top of the valence band. The minimum of the tin $5s$-like band now appears at 5.6 eV above the valence band, suggesting that the donor state repels the host states, increasing the apparent gap. This feature was also observed in the cluster calculations.

In Fig. 4, the total density of states of antimony-doped tin oxide is shown. The p-band-width is found to be 8.1 eV, with three major peaks at 4.3, 7.5, and 10.3 eV. The peaks have changed very little from the position of the peaks for pure tin oxide, and agree very well with the peaks observed by Cox *et al.*[8] Considering the antimony concentration assumed in this work, it is rather a very minor perturbation. It is then not surprising that the UPS measurements indicate almost no change in the valence-band region with antimony doping. The bandwidths of the oxygen $2s$-like band and tin $4d$-like band are found to be 3.6 and $\sim$1.0 eV, respectively, the corresponding energy gaps being 7.3 and 1.7 eV. The two d-like bands due to tin and antimony are separated by $\sim$8.0 eV, which compares well with the x-ray photoemission spectroscopy (XPS) data.

IV. CONCLUSION

In this paper, an attempt has been made to develop a coherent picture of the electronic structure of antimony-

doped tin oxide by first-principles calculations. Using the energy eigenvalues, we have provided a satisfactory explanation of the experimentally observed electronic structure of this material, namely the UPS peaks and the optical gap. It is shown that the positions of the peaks in the density of states with respect to the Fermi surface in the case of antimony-doped material, or with respect to the bottom of the conduction band for the pure tin oxide, remain nearly identical. This is responsible for nearly identical UPS spectra for the pure and antimony-doped materials. A nearly identical picture emerged from the cluster calculations.

The metallic nature of the electrons led to the conclusion that the conductivity is due to the tin 5*s*-like band. Our calculation suggests, at least for systems with high concentrations of antimony, that the impurity band has a nearly free-electron-like structure and can in principle behave like a half-filled metallic band. Additionally, the conductivity of this material will increase with thermal excitation of electrons to the tinlike bands. This, in addition, can lead to absorption of excitation near 1.5 eV resulting in a blue coloration.[9] An alternative explanation based on surface plasmons has been presented on the basis of electron-energy-loss spectroscopy measurements.[9] They are not necessarily mutually exclusive and may contribute conjointly to the coloration of the material.

It has been shown that neither a pure ionic model nor a semiconductor model is adequate to explain the behavior of antimony-doped SnO_2. For such systems, one needs detailed electronic-structure calculations to build a reliable picture of the electronic structure of the material from the experimental observations.

ACKNOWLEDGMENT

The authors wish to thank Dr. B. G. DeBoer from OSI, Towanda for many helpful discussions.

[1]Z. M. Jarzebski and J. P. Marton, J. Electrochem. Soc. **123**, 199c (1976); **123**, 299c (1976); **123**, 333c (1976).
[2]R. E. Aitchison, Aust. J. Appl. Sci. **5**, 10 (1954).
[3]J. McAteer, J. Chem. Soc. Faraday Trans. I **75**, 2762 (1979).
[4]K. Wakabayashi, Y. Kamiya, and H. Ohta, Bull. Chem. Soc. Jpn. **40**, 2172 (1967).
[5]F. J. Berry, Adv. Catal. **30**, 97 (1982).
[6]F. J. Berry and B. J. Laundy, J. Chem. Soc. Dalton Trans. **1981**, 1442.
[7]P. A. Cox, R. G. Egdell, C. Harding, A. F. Orchard, W. R. Patterson, and P. J. Tavener, Solid State Commun. **44**, 837 (1982).
[8]P. A. Cox, R. G. Egdell, C. Harding, W. R. Patterson, and P. J. Tavener, Surf. Sci. **123**, 179 (1982).
[9]R. G. Egdell, W. R. Flavell, and P. Tavener, J. Solid State Chem. **51**, 345 (1984).
[10]F. J. Arlinghaus, J. Phys. Chem. Solids **35**, 931 (1974).
[11]J. A. Jacquemin and G. Brodure, J. Phys. Chem. Solids **12**, 4767 (1979).
[12]J. Robertson, J. Phys. C **12**, 4767 (1979).
[13]E. E. Kohnke, J. Phys. Chem. Solids **23**, 1557 (1962).
[14]M. Nagasawa and S. Shinoya, Phys. Lett. **22**, 409 (1966).
[15]T. L. Credelle, C. G. Fonstad, and R. H. Rediker, Bull. Am. Phys. Soc. **16**, 519 (1971).
[16]J. E. Houston and E. E. Kohnke, J. Appl. Phys. **36**, 3931 (1965).
[17]J. L. Jacquemin, C. Alibert, and M. DeMurcia, Phys. Status Solidi **51**, K75 (1972).
[18]K. C. Mishra, P. C. Schmidt, K. H. Johnson, B. G. DeBoer, J. K. Berkowitz, and E. A. Dale, Phys. Rev. B **42**, 1423 (1990); K. C. Mishra, K. H. Johnson, P. C. Schmidt, B. G. De Boer, J. Olsen, and E. A. Dale, *ibid.* **43**, 14 188 (1991).
[19]R. Wyckoff, *Crystal Structure* (Wiley, New York, 1963), Vol. 1.
[20]J. C. Slater and K. H. Johnson, Phys. Rev. B **5**, 844 (1972); K. H. Johnson and F. C. Smith Jr., *ibid.* **5**, 831 (1972).
[21]A. R. Williams, J. Kübler, and C. D. Gellat Jr., Phys. Rev. B **19**, 6094 (1979).
[22]L. Hedin and B. I. Lundquist, J. Phys. C **4**, 2064 (1971).
[23]P. L. Gobby and G. J. Lapeyre, in *13th Conference on the Physics of Semiconductors,* edited by F. G. Fumi (North-Holland, Amsterdam, 1976).